Jurnal Teknologi

Full Paper

STRUCTURAL SEISMIC PERFORMANCE OF REINFORCED CONCRETE BLOCK SYSTEM FOR TWO STOREYS SAFE HOUSE

Chun-Chieh Yip*, Abdul Kadir Marsono

Faculty of Civil Engineering, Universiti Teknologi Malaysia, 81310 UTM, Johor Bahru, Johor, Malaysia

*Corresponding author
junjiemyx@gmail.com

Article history
Received
4 August 2015
Received in revised form
25 August 2015
Accepted
15 January 2016

Graphical abstract

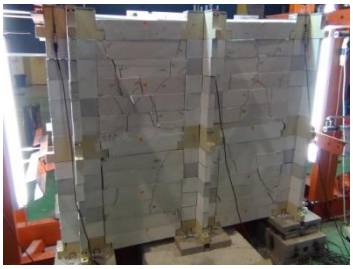

Abstract

Severe earthquakes in year 2004 had caused a destructive tsunami and killed more than 170,000 people in Aceh Indonesia. The disaster raises the public awareness and demand in safe house. This paper presented the structural failure behaviour, strength and performance level of two-bays double storeys safe house structure with the scaled of 1:5. Cyclic pushover test was conducted with compliance to the standard guidelines from Federal Emergency Management Agency (FEMA 356) in year 2000. The structural behaviour and deformation patterns under repeated cyclic lateral loads were identified through experimental test. The structural stiffness capacity, performance level, seismic energy dissipation and spectral acceleration of the safe house model were obtained through calculations from the hysteresis curves. Experimental result shows the ultimate lateral load of safe house model was 9.9 kN with roof top displacement of 49.1 mm. The model has performance level of Immediate Occupancy (IO), Life Safety (LS) and Collapse Prevention (CP) at 6.3 mm, 16 mm and 49.1 mm roof top displacement, respectively. It was found that, the safe house structure is able to withstand seismic excitation of 0.98 g spectral acceleration.

Keywords: Pushover test, concrete block system, safe house, hysteresis curves

Abstrak

Bencana gempa bumi pada tahun 2004 telah menyebabkan tsunami yang teruk dan membunuh lebih daripada 170,000 orang di Aceh Indonesia. Bencana ini telah meningkatkan kesedaran awam dan permintaan ke atas rumah selamat. Kertas ini membentangkan kelakuan kegagalan struktur, kekuatan dan tahap prestasi dua ruang dua tingkat struktur rumah selamat yang berskala 1:5. Ujian kitaran penolakan telah dijalankan dengan mematuhi garis panduan dari Agensi Pengurusan Kecemasan Persekutuan (FEMA 356) pada tahun 2000. Kelakuan struktur dan corak ubah bentuk di bawah beban sisi kitaran berulang telah dikenal pasti melalui ujian makmal. Kapasiti kekakuan struktur, tahap prestasi, pelepasan tenaga seismic dan pecutan spektrum model rumah selamat telah diperolehi melalui pengiraan daripada lengkung histerisis. Keputusan ujikaji makmal menunjukkan beban sisi muktamad untuk rumah selamat adalah 9.9 kN dengan anjakan bumbung sebanyak 49.1 mm. Model ini mempunyai tahap prestasi Penghunian Segera (IO), Keselamatan Hayat (LS) dan Pencegahan Keruntuhan (CP) dengan anjakan bumbung 6.3 mm, 16 mm dan 49.1 mm, masing-masing. Ia telah mendapati bahawa, rumah selamat ini mampu menahan pengujaan seismik sebanyak untuk 0.98 g pecutan spektrum.

Kata kunci: Ujian penolakan, blok konkrit sistem, rumah selamat, lengkung histerisis

1.0 INTRODUCTION

Multiple disasters were happened around the world in year 2012 and 2013 such as serious flooding in Thailand, strong earthquake in Haiti and high frequency tornadoes in United States [1]. The recent earthquakes in Sumatera, Indonesia on 11th April 2012 have reached to a magnitude of 8.6 Richter scale [2]. Fortunately, it only triggers panic without tsunami occurrence, due to the epicentre is located 610 km away from Banda Aceh Indonesia, on the Indo-Australian plate.

In fact, earthquake disaster can cause multiple undesirable structural failures due to liquefaction of the ground soil, landslides, tsunami, and fire crisis. The consequences of these failures are the loss of human life and properties [3]. For example, an earthquake with a magnitude of 8.0 occurred in Sichuan China inland province had caused over 21500 human casualties. The causes of fatality are mainly due to structural failure and liquefaction of the ground soil [4]. Fortunately, Malaysia does not suffer serious earthquake impact so far. However, according to Balendra and Li [5], there were several tremors felt on tall building in Kuala Lumpur due to severe earthquakes occurred in Sumatera. Hence, serious actions have to be taken into considerations to reduce all the impact and negative effect of the earthquake occurrence.

Safe house is invented and acted as an emergency shelter for undesirable natural disaster or man-made hazard [6]. Constructing emergency shelter is a common practice to save people from hurricane and tornado in the state of Florida in the United States of America (USA) [7]. Figure 1 shows an emergency shelter developed by the Federal Emergency Management Agency (FEMA) in USA for sheltering people from hurricane or tornado.

Figure 1 FEMA safe room construction [7]

In China, Lu *et al*. [8] have carried out research on design and optimize emergency shelter for coal mining workers if earthquake strikes. The designed shelter is able to withstand extreme blast impact, shock fragmentation and poisonous gas caused by the explosion [8]. The shelter is equipped with an air filtration system, sufficient food and water supply for survivors.

Bradford and Sen [9] from University of South Florida, USA also invented an emergency shelter for refugees after disaster. The construction of this emergency shelter utilised lightweight and non-corrosive material such as fiber reinforced polymer stud in the wood frame, light weight steel frame and fiber board composite panel as the wall system. This emergency shelter is suitable to be used in hurricane devastated regions. It is able to withstand up to 222.1 km/h wind speed as determined by American Society Civil Engineering (ASCE) 1998 [6]. The erection time of the structure is one to four hours with the aid of an instruction manual. Each component had maximum weight of 355.4 N and is able to be erected by two females. This emergency shelter is usable up to five years depending on the level of maintenance [9].

Texas Tech University had taken initiative in designing their safe room in residential houses with similar concept as shown in Figure 1 and also published standard guidelines for Federal Emergency Management Agency (FEMA) for performance criteria in FEMA 320 [10]. Texas Tech University had successfully tested various types of flying debris with different wind speed on to the safe room. The safe room was constructed by reinforced concrete masonry blocks with grout and anchor lock between the slab, wall and roof [11]. Nevertheless, this safe room concept is still evolving and applied into other field of research such as seismic resistance safe house.

This paper utilises pushover analysis in experimental test to access the safe house structural behaviour and capacity. Pushover analysis is defined as an idealized structure with an assembly of components which is capable to represent the nonlinear monotonic load-deformation characteristics [12]. Pushover test is carried out by applying an invariant lateral load pattern or monotonically load pattern towards the structure or frame [13]. The monotonic lateral load is applied together with constant gravity load, dead load and live load. The test ends with large inelastic deformation occurs on the structure until the targeted value is reached. The main purpose of the pushover test is to push the structure to until the expected maximum targeted displacement. This test is known as drift versus force demand evaluation and component deformation assessment [14]. In short, standard pushover test is able to assess the non-linearity of the structure behaviour and obtain hysteresis curve in terms of shear-force versus displacement realistically. The weak point of the structure can be easily identified throughout the check of progressive damage in relation to roof top displacements in the cyclic pushover test [3]. Hence, the elastic and plastic behaviour of the structure can be determined through

pushover hysteresis curve. The procedure to conduct a pushover test is available in FEMA 273 [14] and 356 [15]. A standard theoretical prediction of targeted displacement from FEMA 440 is needed for an experimental test [16].

In conventional concrete structural code of practice, only linear elastic limit states of structure are taking into considerations. However, in seismic resistance structure design, their performances are accessed more quantitatively into inelastic states. In seismic design, the performance of the structure is able to predict with sufficient data from intensity of earthquake ground motion, building site and design life. Structural seismic performance levels are evaluated in terms of damage that coupled with the level of earthquake hazard [17].

Performance based seismic design compliance with FEMA 273 [14] needs to be assessed to determine the current structure seismic performance level [9].The building performance levels introduced by FEMA 273 [14] are categorised into four different levels which are known as Operational, Immediate Occupancy (IO), Life Safety (LS) and Collapse Prevention (CP) as shown in Figure 2. Each level of performance has different damage identification in the structural system or elements.

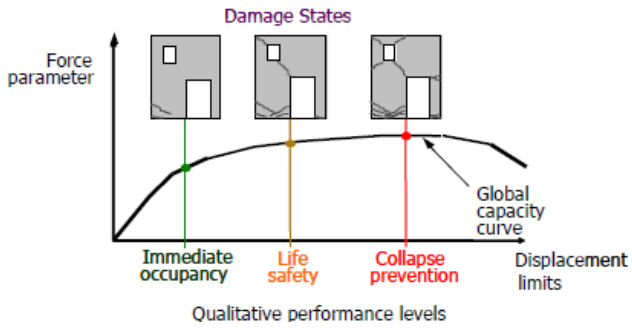

Figure 2 Structural qualitative performance level [14]

In IO performance level, the structure remains safe for occupant. In this level, very limited structural damage and risk of life are occurred. The structure can be reoccupied right after the earthquake disaster with some minor repairs [15]. Structure performance level of LS means significant structural damage has occurred after the earthquake disaster. Some structural components and elements are severely damaged without falling debris hazards. Stiffness of the structure may be degraded, but still retains marginal strength from total collapse. Light injuries and low risk of life threatening may occur during the earthquake. The structure can be repaired and reoccupy after the earthquake, but the repairing cost is very high [15]. In CP stage, the structure is on the verge of partial or total collapse. Stiffness of the structure is reduced to critical stage with large permanent lateral deformation of the structure. The structure loses its lateral resistance. Risk from debris falling hazard may exist in CP stage. The structure cannot be repaired or reoccupied after the earthquake disaster [15].

Hence, the identification of structural performance level can be performed with sufficient information and guideline for structural damages assessment recorded throughout the experimental test. Again, the structural damage is determined from range of local damage up to global damage parameters.

Full scale experimentations for this model are costly and time consuming. Hence, this paper presents a down scaled 1:5 experimental model to investigate seismic demand on building by controlled displacement cyclic lateral load test. The failure mechanism and structural movement patterns were obtained to determine the structural performance level.

2.0 EXPERIMENTAL DETAILS

2.1 Specimen Specifications

Structural specifications of safe house with the scale of 1:5 are shown in Figure 3. Ten types of IBS block work structural components were used in this research. Square blocks, rectangular blocks, T-blocks, L-blocks, beam blocks, wall infilled blocks and slab blocks are part of the structure. These individual structural components were used to construct two bay double storeys safe house with 1.48 meter height, 0.74 meter width and 1.48 meter length as shown in Figure 3(a). Each type of the concrete block has its unique reinforcement design as shown in Figure 3(b). Concrete blocks were joined together by bolts and nuts. The foundation of safe house was fabricated separately for supportive purposes.

Total of four hundred and nine small components were fabricated in the laboratory for the assembly of this structure. The calculated overall structural weight was 1014.3 kg ≈ 1 ton. The details of components shapes are shown in Table 1. Sixty rectangular blocks and 180 square blocks were assembled to construct 6 columns. Six T-Blocks (Big) and 18 T-Blocks (Small) were placed at foundation level. T-Block acts as support for columns and ground beams.

Twelve L-Blocks (Big) and 36 L-Blocks (Small) were placed at first and roof floor column. L-Blocks were placed on top of the column to support the roof beams. The main function of L-Blocks is to provide supports for both beams and slabs. From Table 1, 21 beams were fabricated to support slabs and wall infill. Two slabs type A and four slabs type B were combined and placed together on second floor of the safe house structure as shown in Figure 3(a).

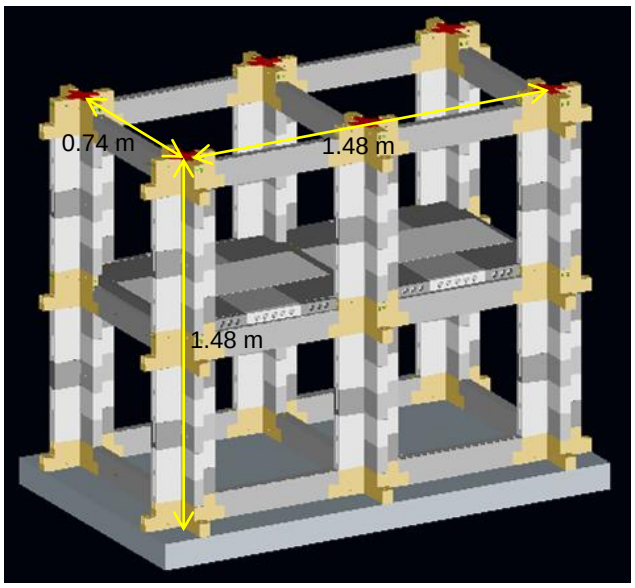

(a)

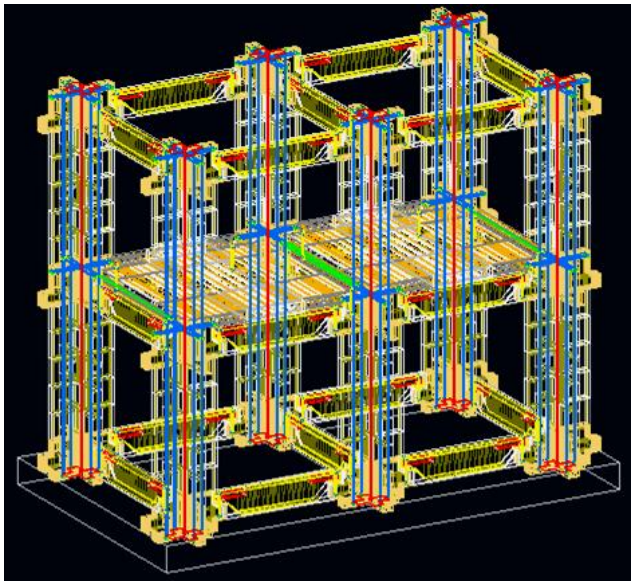

(b)

Figure 3 Illustration of proposed safe house (a) Perspective view of safe house, (b) Reinforcement details

Table 1 Safe house structural component details

Description	Components Photos	Dimension (mm)	Required Components
Rectangular Block	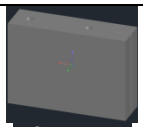	100x140x40	60
Square Block		100x100x40	180
T-Block (Big)		180x140x40	6
T-Block (Small)	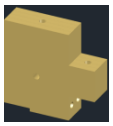	140x140x40	18
L-Block (Big)		180x140x40	12
L-Block (Small)		140x140x40	36
Wall Infill (Replaced by aerated concrete)		500x100x40	70
Beam Block		500x100x40	21
Slab A	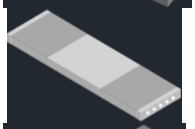	740x220x40	2
Slab B		740x260x40	4
Total fabricated components			409

2.2 Reinforcements Specification

All the reinforcements were designed by IBS research group as compliance with European code 3 [19] and British standard BS5950 [20] only. Reinforcements with diameter of 1.5 mm, 3.0 mm and 6.0 mm were used for down scaled 1:5 specimen components fabrication in this research. Reinforcement with a diameter of 3.0 mm was used to fabricate T and L blocks with specific dimension as shown in Figure 4. It should be noted that all dimensions in Figure 4 are in millimetre. The T and L block reinforcements were made by several continuous loops and tightened by steel wire. This technique was also applied no the square and rectangular blocks.

Steel bar of 6 mm diameter was used to fabricate the beam main reinforcement according to specified dimensions as shown in Figure 5. The continuous shear link with 20 mm of spacing on the beam main reinforcement was made by 1.5 mm steel bar. The continuous shear link and main reinforcement were bonded together by steel wire. Spiral or continuous shear links were excellent in distributing shear force along the main reinforcement in the beam. Two C-shape steel plates with thickness of 1.5 mm, width of 15 mm and length of 220 mm were placed at both

ends of the beam main reinforcement as anchor plates shown in Figure 5. The purposes of these two c-shape plate are to grip the bolts and nuts together and prevent the beam from falling apart when the beam-column concrete joint failed.

Steel bar with diameter of 3 mm was used for fabrication of slab reinforcement as shown in Figure 6. The reinforcement of the slab was made into C-shape. The C-shape steel reinforcement was excellent in distributing compressive force coming from the top and resisting tensile force from the bottom.

The spacing of C-shape steel reinforcement was 32.5 mm. The purpose of spacing the reinforcement is to create empty cylindrical hole in between reinforcement to reduce overall weight and serve as utilities hole. Top layer C-shape reinforcement for compressive resistance was having 220 mm in length measured from side to middle. The purpose of not overlapping the top side reinforcement is to provide certain level of ductility in the slab. If failure such as minor cracks occurs, it can be detached earlier and take action to retrofit or replace the damaged component.

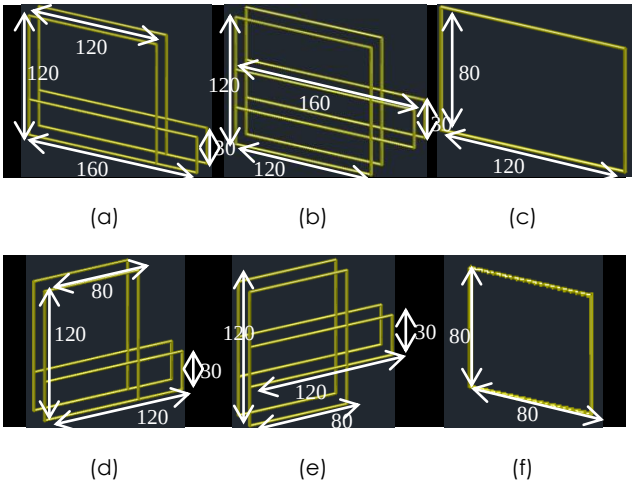

Figure 4 Reinforcement details (a) L-Big, (b) T-Big, (c) Rectangular, (d) L-Small, (e) T-Small and (f) Square

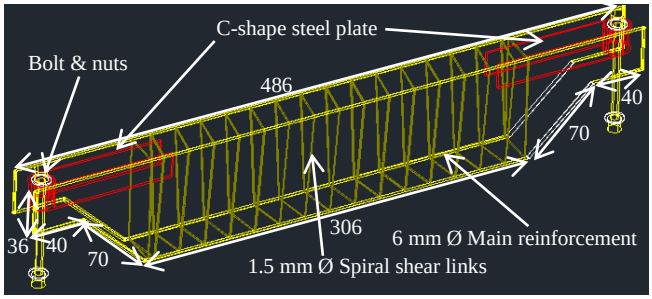

Figure 5 Reinforcement details for beam

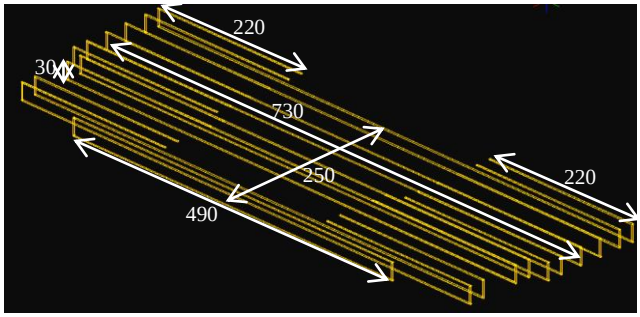

(a)

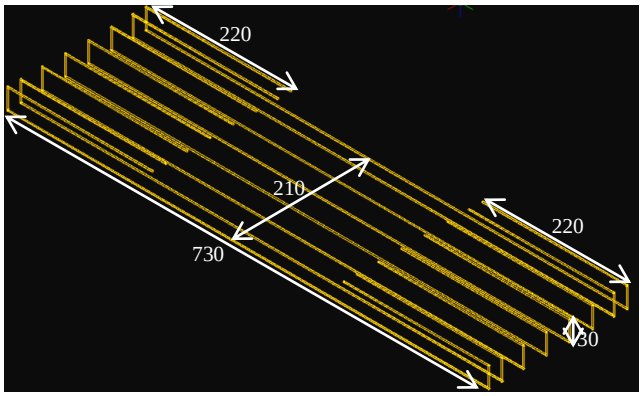

(b)

Figure 6 Reinforcement details for slabs type (a) and type (b)

Tensile test for steel bar with diameter of 1.5 mm, 3.0 mm and 5.0 mm were carried out in Mechanical Laboratory of Universiti Teknologi Malaysia. The details and material properties for steel bar diameter of 1.5 mm, 3.0 mm and 5.0 mm were listed in Table 2, Table 3 and Table 4 respectively. Steel bar with 1.5 mm in diameter has average yield stress of 919.4 MPa and average modulus elasticity of 227.0 GPa. For steel bar with 3.0 mm in diameter, the average yield stress was 676.7 MPa and average modulus of elasticity was 217.4 GPa. Steel bar with 5.0 mm in diameter was having yield stress of 549.8 MPa and modulus elasticity of 209.7 GPa.

Table 2 Characteristic Tensile strength of diameter 1.5 mm steel reinforcement

Diameter of steel bar	Yield Load, (kN)	Yield Stress, (MPa)	Ultimate Load, (kN)	Maximum Stress, (MPa)	Maximum Strain, (mm/mm)	Modulus of Elasticity, (GPa)
1.5mm	1.636	926.14	1.705	965.309	0.01179	226.169
1.5mm	1.637	926.86	1.715	970.444	0.01539	228.641
1.5mm	1.607	909.57	1.682	952.245	0.01803	226.005
1.5mm	1.617	915.12	1.692	957.969	0.01604	227.218
Average	1.624	919.42	1.698	961.491	0.01531	227.008

Table 3 Tensile strength of diameter 3.0 mm steel reinforcement

Diameter of steel bar	Yield Load, (kN)	Yield Stress, (MPa)	Ultimate Load, (kN)	Maximum Stress, (MPa)	Maximum Strain, (mm/mm)	Modulus of Elasticity, (GPa)
3.0mm	4.810	680.51	5.109	722.810	0.05161	229.240
3.0mm	4.807	680.13	5.078	718.372	0.03314	211.839
3.0mm	4.732	669.55	5.004	708.058	0.03356	211.211
Average	4.783	676.73	5.064	716.413	0.03944	217.430

Table 4 Tensile strength of diameter 5.0 mm steel reinforcement

Diameter of steel bar	Yield Load, (kN)	Yield Stress, (MPa)	Ultimate Load, (kN)	Maximum Stress, (MPa)	Maximum Strain, (mm/mm)	Modulus of Elasticity, (GPa)
5.0mm	17.08	664.91	17.580	684.144	0.03570	209.902
5.0mm	12.85	517.97	13.308	536.504	0.01514	226.549
5.0mm	13.21	528.55	13.596	544.211	0.02456	217.317
5.0mm	13.09	524.16	13.600	544.349	0.03217	211.355
5.0mm	12.83	513.58	13.570	543.166	0.03239	183.624
Average	13.81	549.83	14.331	570.475	0.02799	209.749

2.3 Concrete Mix Specification

Quantity of 1 m^3 concrete mix design for safe house was shown in Table 5. The concrete mix was designed for characteristic strength of 30 N/mm^2 at 28 days based on the British Standard BS5328: Part 2: 1997. Total of 19 concrete cylinders were tested for material concrete compressive and tensile strength is shown in Table 6. The average concrete compressive strength and tensile strength obtained from laboratory tests were 33.97 N/mm^2 and 4.81 N/mm^2 respectively. Based on the mix design shown in Table 5, the obtained modulus of elasticity for 28 days concrete cylinder samples was 37496.91 N/mm^2 as shown in Figure 7.

Table 5 Mixture of concrete for safe house

Water / Cement ratio	Cement (kg/m^3)	Water (kg/m^3)	Fine Aggregate (kg/m^3)	Coarse Aggregate (kg/m^3)	Density (kg/m^3)	Admixture 1.2% (kg)
0.42	550.0	233.0	511.0	1086.0	2380.0	6.6

Table 6 Concrete compressive strength f_{cu} & splitting strength f_t of grade C30 concrete

Date of casting	Date of testing	Age (days)	Sample weight, (kg)	Maximum load, (kN)	Maximum stress, (N/mm^2)
					Compressive strength, f_{cu}
25/3/2013	21/4/2013	28	3.700	239.6	30.510
17/4/2013	15/5/2013	28	3.725	259.4	33.020
17/4/2013	15/5/2013	28	3.705	242.1	30.820
18/4/2013	16/5/2013	28	3.695	316.3	40.270

18/4/2013	16/5/2013	28	3.695	264.4	33.670
10/5/2013	7/6/2013	28	3.735	240.1	30.560
17/5/2013	11/9/2013	117	3.700	266.3	33.900
18/6/2013	11/9/2013	85	3.665	324.9	41.360
3/7/2013	11/9/2013	70	3.715	259.5	33.040
3/7/2013	11/9/2013	70	3.715	255.5	32.530
				Average	33.970

Date of casting	Date of testing	Age (days)	Sample weight, (kg)	Maximum load, (kN)	Splitting strength, f_t
25/3/2013	21/4/2013	28	3.770	186.9	5.948
25/3/2013	21/4/2013	28	3.765	181.3	5.772
17/4/2013	15/5/2013	28	3.715	152.4	4.851
18/4/2013	16/5/2013	28	3.680	149.5	4.760
10/5/2013	7/6/2013	28	3.725	132.7	4.223
19/4/2013	11/9/2013	145	3.700	125.1	3.983
17/5/2013	11/9/2013	117	3.680	135.9	4.327
17/5/2013	11/9/2013	117	3.645	115.8	3.688
18/6/2013	11/9/2013	85	3.680	181.9	5.789
				Average	4.815

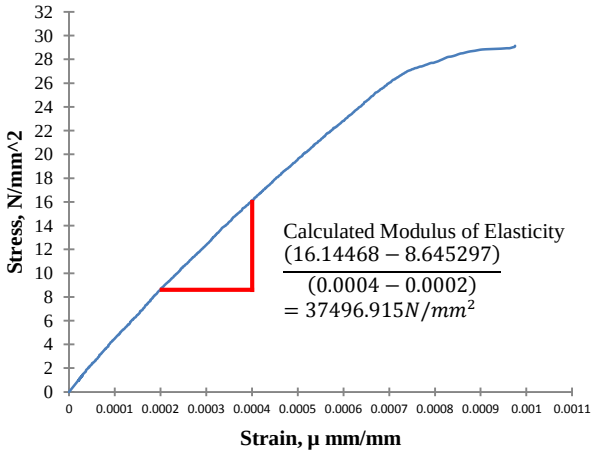

Figure 7 Stress strain curve of concrete grade C30

Figure 8 First floor slabs and live loads

3.0 EXPERIMENTAL PROCEDURE

Structure installation works, setting up test frame and experimental testing were carried out in Structure Laboratory. Before the test was conducted, total of thirty two units of steel mass blocks were placed on top of the safe house slabs as shown in Figure 8. Based on standard requirement of BS6399-1.1996 [21], minimum imposed floor load with partial safety factor of 1.5 for live load action and floor impose load with 32.85 kg in form of mass block was distributed evenly across the floor of the structure.

Before conducting the experiment test, the theoretical targeted roof top displacement was calculated according to FEMA 356 [15] and 440 [16] standard guidelines. The theoretical targeted roof top displacement for first cycle, second cycle, third cycle and fourth cycle test were 6.3 mm, 12.7 mm, 25.4 mm and 47.6 mm respectively. All the calculated theoretical roof top displacements were complied with clause 3.3.3.3.2 target displacement in FEMA 356 [15]. The target displacement δ_t is as shown in Equation 1.

$$\delta_t = C_0 C_1 C_2 C_3 S_a \frac{T_e^2}{4\pi^2} g \quad (1)$$

The annotations in Equation 1 are stated as follow:

C_0 = Modification factor to relate spectral displacement of an equivalent SDOF system to roof displacement of the building. The appropriate value can be obtained in Table 3-2 FEMA 273 [14].

C_1 = Modification factor to relate expected maximum inelastic displacements to displacements calculated for linear elastic response:
= 1.0 for $T_e \geq T_s$
= [1.0 + (R-1)T_s/T_e]/R for $T_e < T_s$ but not greater than the values given in Section 3.3.1.3 nor less than 1.0.

T_e = Effective fundamental period of the building in the direction under consideration with unit in second.

T_s = Characteristic period of the response spectrum, defined as the period associated with the transition from the constant acceleration segment of the spectrum to the constant velocity segment of the spectrum per Section 1.6.1.5 and 1.6.2.1 in FEMA 356 [15].

S_a = Response spectrum acceleration at the effective fundamental period and damping ratio of the building in the direction under consideration, g, as calculated in Section 1.6.1.5 and 1.6.2.1.

g = Gravitational acceleration.

R = Ratio of elastic strength demand to calculated yield strength coefficient calculated by following equation.

$$R = \frac{S_a}{V_y/W} C_m$$

V_y = Yield strength calculated using results of the NSP for the idealized nonlinear force displacement curve developed for the building in accordance with Section 3.3.3.2.4.

W = Effective seismic weight as calculated in Section 3.3.1.3.1.

C_m = Effective mass factor from Table 3-1 FEMA 356 [15]. Alternatively C_m taken as the effective model mass calculated for the fundamental mode using an Eigenvalue analysis shall be permitted.

C_2 = Modification factor to represent the effect of pinched hysteretic shape, stiffness degradation and strength deterioration on maximum displacement response. Value C_2 for different framing systems and structural Performance Levels shall be obtained from Table 3-3 FEMA 356 [15]. Alternatively, use of C_2 = 1.0 shall be permitted for nonlinear procedures.

C_3 = Modification factor to represent increased displacements due to dynamic P-Δ effect. For buildings with positive post yield stiffness, C_3 shall be set equal to 1.0. For building with negative post-yield stiffness, values of C_3 shall be calculated using Equation as follow, but not to exceed the values set forth in Section 3.3.1.3.

$$C_3 = 1.0 + \frac{|\alpha|(R-1)^{3/2}}{T_e}$$

Where R and T_e are as defined above and:
a = Ratio of post-yield stiffness to effective elastic stiffness, where the nonlinear force displacement relation shall be characterized by a bilinear relation as shown in Figure 3-1 FEMA 356 [15].

For the test setup, 7 linear variable displacement transducers (LVDT), one load cell with 5 tons capacity and one data logger were used for experimental testing. Test setup is as shown in Figure 9. Three LVDTs were placed laterally to the structure while the other 3 LVDTs were placed at the top of the structure. One LVDT was place at the opposite lateral side of the structure. Three horizontal LVDTs were responsible to record roof top displacements and intermediate storey displacement. A LVDT was placed at bottom of the structure to make sure the entire structure was remained static during the testing.

Three LVDTs were placed vertically on top of three columns to measure the displacement generated by push and pull forces. All recorded data were stored in a computer. Software TDS-7130 was used for the with data logger.

Three inclinometers were placed at the other three columns as shown in Figure 9 to measure the rotation caused by push and pull effects. A laser distance gauge (LDG) was placed at top right test frame as shown in Figure 9 to counter-measure the recorded displacement beside the roof top LVDTs. Inclinometers and LDG data were recorded manually during the test. The structure was tested up to its ultimate capacity after the targeted displacement in fourth cycle was achieved.

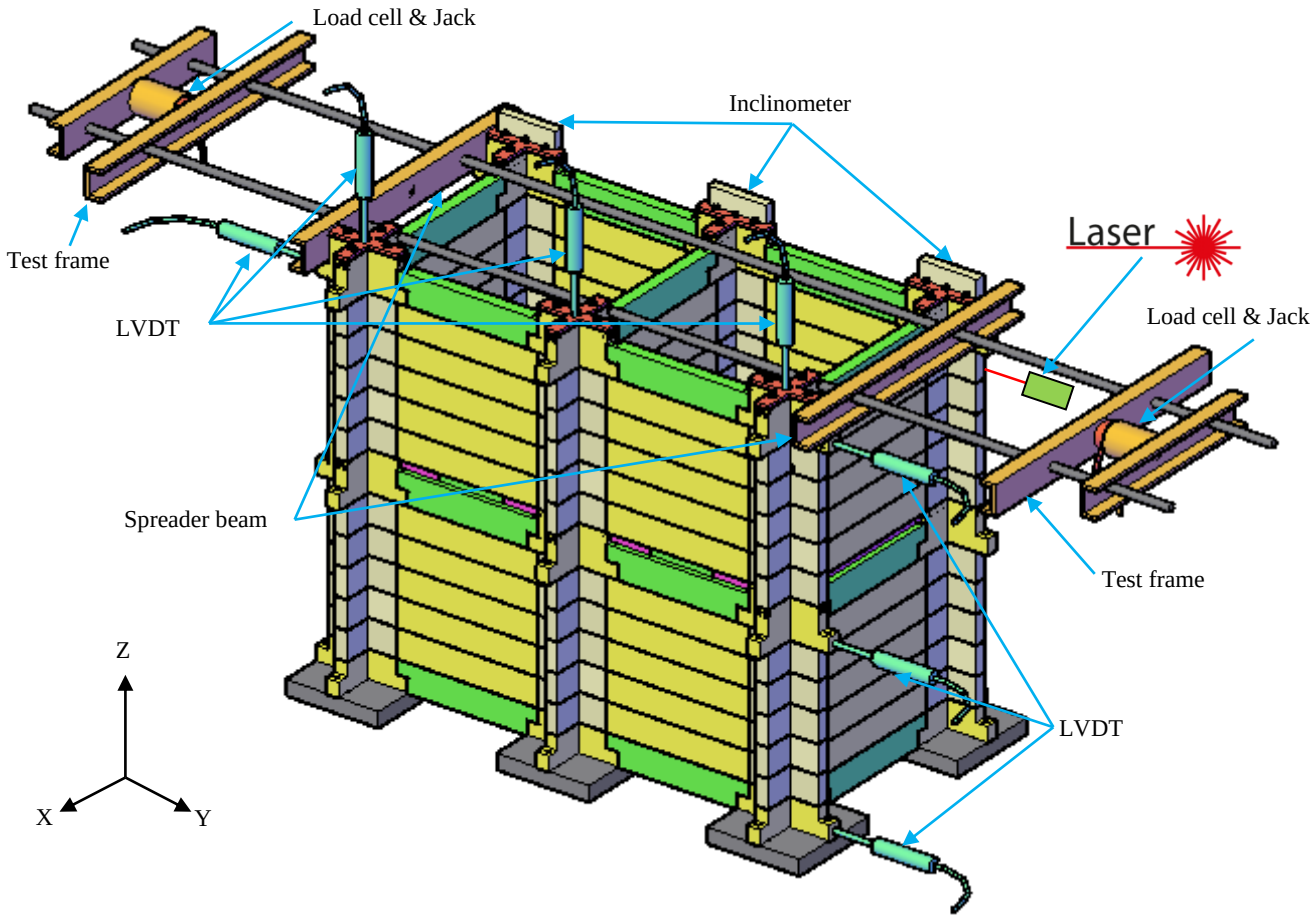

Figure 9 Three-dimensional schematic test setup

4.0 TEST RESULTS AND DISSCUSSION

All the experimental results from cyclic pushover test conducted on scale 1:5 of two storeys and two bays safe house were presented in this paper. The hysteresis curve, structural deformation pattern, capacity curve and energy dissipation curve are briefly discussed in this section. Data recorded from data logger were extracted for the formation of hysteretic curve. Detail damage assessment of the concrete block components were performed in every load cycle test.

4.1 First Cycle Test

The first cycle was started by pushing the structure toward left (negative direction) up to 6.3 mm of roof top displacement. The intermediate displacement data was collected from every cycle until the targeted roof top displacement is reached. This action was to ensure that the deformation sequences of every component were recorded during the test. By completing the first cycle, the structure was again pushed in positive direction (toward right) up to roof top displacement of 6.3 mm. The first cycle only stop after both jacks pressure were released and letting the structure back to its original position.

Figure 10 illustrated the load versus displacement curve was started to increase linearly up until 2.0 mm displacement in negative direction. A progressive curve was formed after 2.0 mm displacement up to the targeted roof top displacement of 6.3 mm. A sharp decrease of linear load versus displacement line was formed due to the release of the jack pressure during the test. This indicates that the structure still behave elastically when it goes back to its original position after the load was released.

The test was continued at positive direction by pushing the structure towards the left side. The load versus displacement curve increased steadily until 6.3 mm displacement with load 2.6 kN of load. Figure 10 shows a steady decrease in load versus displacement curve after the load was released due to the formation of new cracks and blocks rotation. These conditions had caused minor reduction in structural stiffness capacity. Besides, roof top displacement stopped at 1.5 mm which also required an additional applied force to reset the structure back to its original position. This was due to the frictional force generated by the displaced concrete blocks.

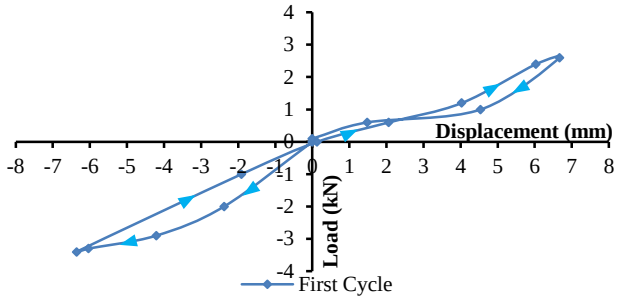

Figure 10 First cycle hysteretic curve

4.2 Second Cycle Test

In Figure 11, the recorded initial displacements of the second cycle test were greater than the first cycle test for both negative and positive directions. For example, first cycle requires 2 kN of load to obtain roof top displacement of 2.4 mm in negative direction. However, in second cycle only 1 kN load was sufficient for obtaining displacement of 2.5 mm in negative direction. This situation indicates that the stiffness of the structure starts to degrade after the first cycle test. As usual the structure was pushed up to the targeted roof top displacement of 12.7 mm. After the jack was released, the structure reversed back to roof top displacement of 4.5 mm. This phenomenon indicates that the structure system still having elasticity. Due to the formation of cracks in the beam and column, the structure system started to lose its internal resistance with formation of permanent storey drift.

The second cycle test was then continued by pushing the structure toward right (positive) direction. The test was continued up to displacement of 12.7 mm with an applied load of 4.5 kN. After the jack pressure was released, the structure reversed back slowly until the roof top permanent displacement of 3 mm. Since the structure does not returned to its original location, an extra 0.6 kN loading was applied to the opposite direction until the roof top displacement reached the origin vertical position.

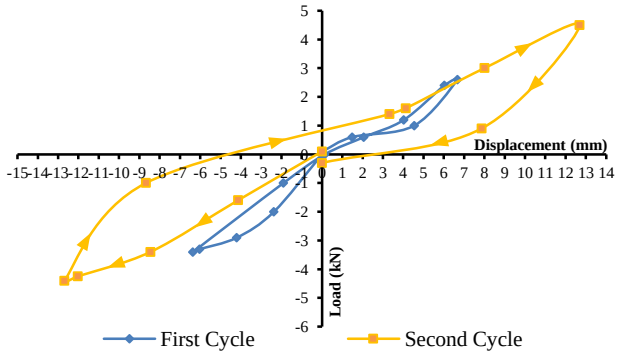

Figure 11 Second cycle hysteretic curve

4.3 Third Cycle Test

The third cycle test was began by pushing the structure towards the negative direction. Through Figure 12, the stiffness of the structure is further degraded throughout the cyclical test. Fortunately, the safe house structural components are still functional after the third cycle test. Initially, third cycle was pushed up to the targeted displacement of 25.29 mm with 7.2 kN load. The structure was stopped at roof top displacement of 5.00 mm after the load from the jack was completely released. Reverse load of 0.8 kN was applied to push back the structure to its original position.

The test was continued by pushing the structure towards the positive direction with roof top displacement of 25.43 mm and load of 5.9 kN. An obvious difference shown in Figure 12 was applied load toward negative direction required 7.2 kN but toward positive direction only 5.9 kN load was used for reaching displacement of 25.4 mm. This phenomenon was due to the damage in beam to column joints and stiffness degradation in columns together with wall elements. The elasticity of the structure was degraded due to the repeated push and pull cyclic load test. Figure 12 indicates that the structure losses its elasticity due to stiffness degradation at recorded roof top displacement of 12 mm after the applied load was fully released at the end of the cycle. Additional 0.3 kN of reverse load was applied to push the structure back to its original position.

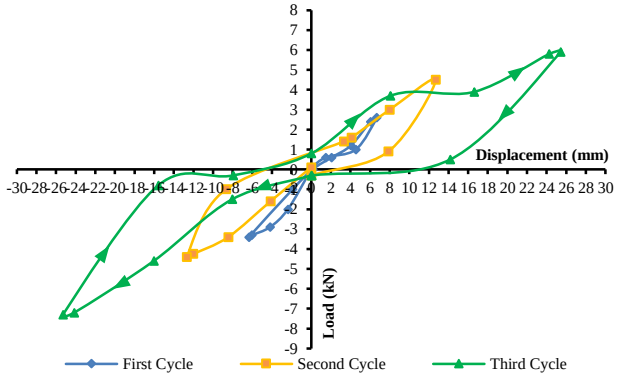

Figure 12 Third cycle hysteretic curve

4.4 Fourth Cycle Test

Fourth cycle test was began by pushing the structure toward negative direction up to roof top displacement of 47.6 mm. The structure ultimate capacity test was launched by pushing toward the positive direction slowly until the structure loses its resistance in the positive direction.

The recorded ultimate lateral load capacity of the structure was 9.9 kN with roof top displacement of 49.1 mm. The test ends at roof top displacement of 58.08 mm with lateral load resistance dropped from 9.9 kN to 6.8 kN. The test was stopped due to the failure of

welded foundations to fixed ground as shown in Figure 13.

In Figure 13, the structure swayed towards the right direction at the end of the test. The recorded roof top displacement at ultimate capacity was 49.1 mm while intermediate storey displacement was 22.1 mm. The recorded data indicates that the first floor columns shown in Figure 13 have more displacement than the ground floor columns. Through the observation from Figure 13, the left side concrete blocks of column A were experiencing separation. However the right side concrete blocks were experiencing sliding effect.

These conditions happened when the left column was experiencing tensile force and the right column was experiencing compressive force. Tensile force in the left column was taken by the column bolt while compressive force at the right side of the column was taken by reinforced concrete blocks. Since the column was made by four parts of concrete blocks, both middle parts of concrete blocks in the column A was taking partial tensile and compressive load together.

Further observation on column B has discovered that the effect of tensile and compressive behaviour were minimised at the centre of the structure. The tensile and compressive behaviours carried from column A have been altered become fully tensile behaviour in column C due to the concrete blocks sliding effect. Hence, all the loadings in column C were taken by five bolts in the column.

For ground floor condition, only concrete T-blocks at far end of left and right sides were crushed by excessive compressive load during the cyclical test as shown in Figure 13. The crushed parts were mostly concrete fire prove cover. The confined reinforced concrete core was still functional. The remaining damages on all six columns were formation of plastic hinges at beam-column connections.

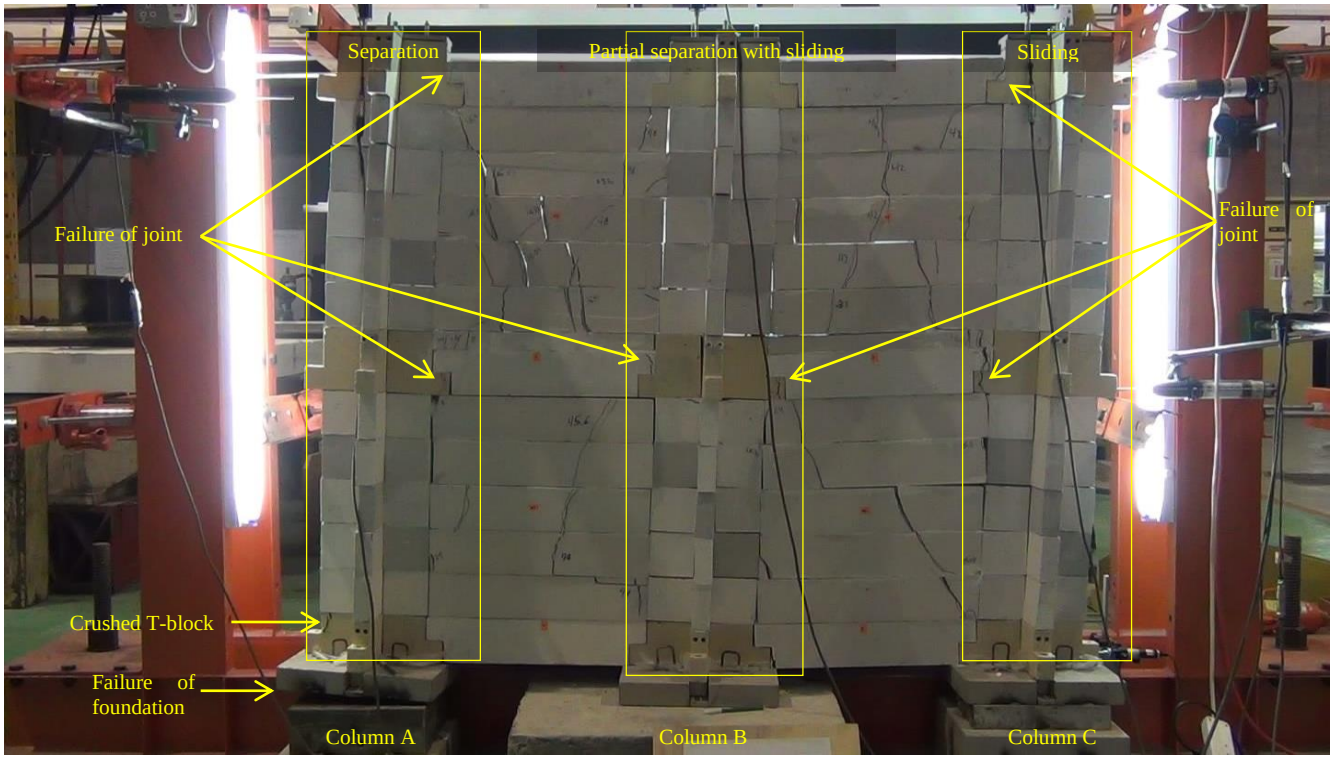

Figure 13 Front view structural behaviour of fourth cycle test

In fourth cycle test, the structure was pushed towards negative direction. The structure began to experience sliding effect when the horizontal load was applied as shown by the light blue line stared from 0 mm displacement to 15 mm in Figure 14. These large displacements were generated by the frictional force in between every concrete blocks. The structural bolts were taking loadings from the 15 mm displacement up to 47.6 mm with loading of 9.1kN for first half of the cycle test. Many cracks were formed on the walls and corbel of L-blocks when the structure was pushed up to 42 mm displacement. The structure was returned back and stopped at the roof top displacement of 14 mm after the load from jack was completely released.

The experiment proceeds by pushing the structure toward the positive direction for the ultimate capacity test. Additional loads of 2 kN was applied to push the structure back to the original position. Again, the frictional resistance took part from load 0 kN up to 4 kN with roof top displacement of 15 mm. The tested ultimate capacity of the structure was 9.9 kN with 49.1 mm displacement. The curve marked with red line in Figure 14 indicates the structure loss its resistance due to the failure of footing.

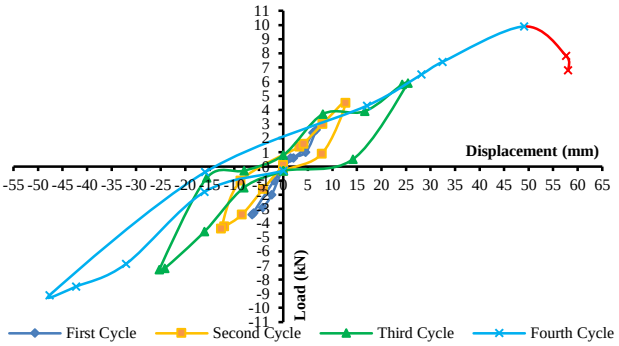

Figure 14 Fourth cycle hysteretic curve

4.5 Structural Stiffness Capacity

Figure 15 shows the structural stiffness capacity curve in negative direction and idealized bilinear curve. Identification of the bilinear curve was to measure the structural effective stiffness and structural post-yield stiffness capacity. From the stiffness capacity curve the structure has initial stiffness K_i of 0.8823 kN/mm as shown in Figure 15.

The structure was in elastic state with base shear up to 2.5 kN in the negative direction. The structure has permanent drift when the base shear exceeded 2.5 kN. Larger permanent storey drift and stiffness degradation occurred after the base shear beyond 7.2 kN. Maximum recorded structural base shear, V_t in the negative direction was 9.1 kN with storey drift, δ_t of 47.62 mm as shown in Figure 15. An idealized bilinear curve was plotted based on equal energy rule. Equal energy rule is known as area above and below the curve that is approximately balance. Through normalized bilinear curve shown in Figure 15, effective yield strength V_y of the structure was 6.7 kN with displacement of 16 mm. The calculated effect stiffness K_e under 60 % of the effective base shear force 4.02 kN was 0.375 kN/mm. Other than that, the calculated effective post yielding structural stiffness, αK_e was 0.0892 kN/mm.

From Figure 16, the initial structural stiffness K_i in positive direction was 0.4286 kN/mm. In comparison between the negative and positive direction, negative direction has higher initial structural stiffness capacity. The recorded maximum base shear, V_t was 9.9 kN together with storey drift, δ_t of 49.09 mm in the positive direction. From the idealized bilinear curve plotted in Figure 16, it shows the effective yielding strength, V_y in positive direction of the structure was 5 kN with yielding drift of 14 mm. The effective structural stiffness, K_e under 60 % of the effective base shear of 3 kN was 0.3333 kN/mm. Besides, the structural effective post yielding stiffness, αK_e in the positive direction was 0.1428 kN/mm. From the calculated αK_e in both directions, the structure pushed towards the positive direction experiencing yielding earlier than in the negative direction. The calculated effective stiffness, K_e of 0.3 kN/mm in both negative and positive direction was almost similar. This indicates the structure has similar effective stiffness capacity in both loaded directions. All these calculated parameters were able to become an input into finite element for further analysis and provide insight for reader to understand at what level the structure retain or loss its stiffness capacity.

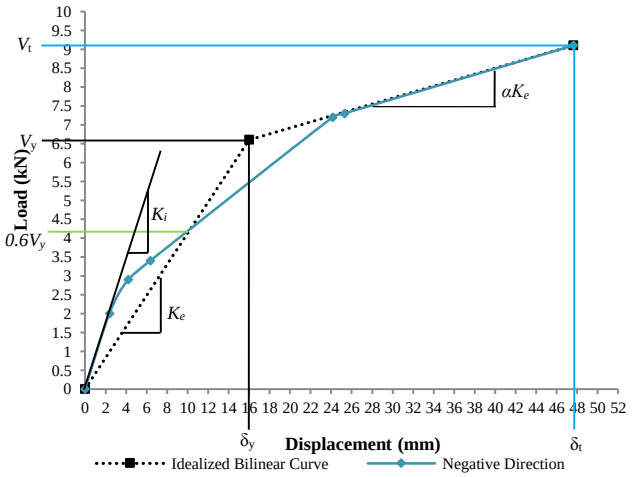

Figure 15 Idealised force versus displacement curve in negative direction

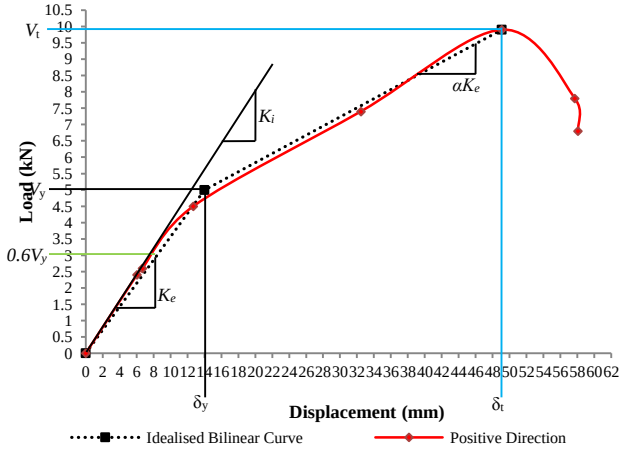

Figure 16 Idealised force versus displacement curve in positive direction

4.6 Structural Performance Level

Figure 17 shows the capacity curve of the safe house model. From the experimental test, the structure was in Immediate Occupancy performance level at storey drift of 6.3 mm with base shear of 3.4 kN as shown in Figure 17. In Immediate Occupancy stage, the structure had suffered light damage, no permanent drift, retained original strength and stiffness. Only minor cracks on facades of square, rectangular and wall blocks were discovered without crushing during the test. All structural components were still functional and

able to reoccupy even after an earthquake had occurred.

The limit of Life Safety performance level for the safe house structure was extended up to the storey drift of 16.0 mm with 5.3 kN base shear as shown in Figure 17. During the Life Safety performance level, moderate damage on wall, L-blocks, T-blocks, beams, rectangle and square blocks were occurred throughout the cyclical load test. The damages were including with minor spalling of concrete cover, increased in crack opening and crack length. In this stage, permanent drift was formed due to the degradation of structural stiffness strength. For wall elements, no out of plane and diagonal cracks were formed at this performance level. In this damage control range, minimal repair on damaged structural was essential to protect and preserve the structural elements from environmental attack after earthquake. The safety of occupants was still protected by the structure without any injuries or harms caused by the structural failure.

In Figure 17 the limit of Collapse Prevention performance level was located at storey drift of 49.1 mm with maximum base shear of 9.9 kN. In this performance level, formations of plastic hinges occurred at the beams to columns joint. Apart from that, T-blocks in the foundation were crushed by excessive compressive load generated during the cyclical load test. Diagonal cracks, severe spalling and large concrete crack were formed up to this performance level. The stiffness capacity of the safe house structure was further degraded by excessive damage. There are possible debris falling hazards from concrete cover and wall in this performance level. The formation of plastic hinge at the beam to column joints were protected by the internal steel anchor, thus preventing the beam from complete detached from the structure. The steel anchor in the beam to column joints were the final defence for protecting occupant during evacuation from the structure. This structure has tendency to collapse in this performance level.

Beyond Collapse Prevention performance level was the structural collapse hazard. In this collapse stage, the safe house structure was losing its stiffness capacity with incremental storey drift. The structure was collapsed due to the dislocation of the foundations and failure of the column bolts. Dislocation of foundations may caused by liquefaction of soil in the event of earthquake. Safe house structure was designed based on strong column weak beam concept. Hence, the failure of the column bolts also cause the total collapse of the structure.

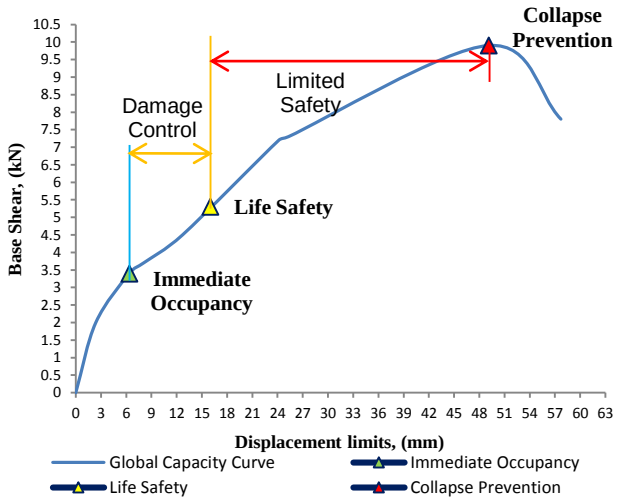

Figure 17 Structural qualitative performance levels based on storey drift

4.7 Structural Seismic Energy Dissipation

Figure 18 shows calculated energy dissipation curve at every cycle load test. The energy dissipation curve was calculated based on the area within the hysteresis loop. The area within the hysteresis loops was calculated manually on graph paper for every cycle test. Not much energy dissipation was recorded in negative direction with 3.1 kNmm and 1.6 kNmm in positive direction for the first cycle test. In the second cycle test, negative direction has higher energy dissipation capability of 21.5 kNmm. However, only 18.5 kNmm of energy was dissipated in positive direction for the second cycle test. Energy dissipation was increased up to 62.0 kNmm for positive direction and overtaken 48.5 kNmm energy dissipated in the negative direction for the third cycle test. The rate of energy dissipation was based on the ductility of the structure. When the structural stiffness capacity was reduced, more earthquake energies were dissipated through the beam to column joints and other structural components.

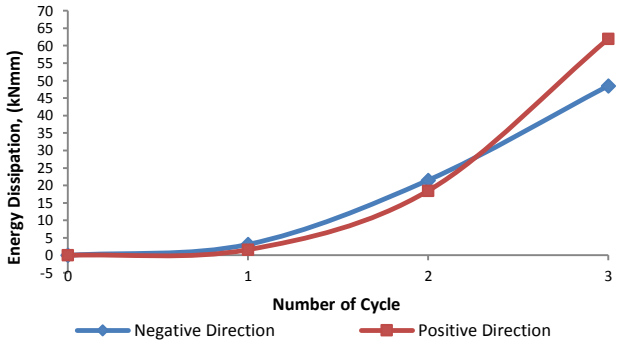

Figure 18 Energy dissipation curve in every cycle test

4.8 Spectral Acceleration of Safe House Model

The spectral acceleration of the structure in Table 7 can be calculated by dividing the maximum base shear in every cycle to the structure weight. The calculated overall structural weight was 1014.3 kg. The calculated spectral acceleration was closely related with structural performance level. The findings of this research are the safe house structure with Immediate Occupancy performance level are able to sustain earthquake ground motion intensity up to 0.33 g defined in the spectral acceleration. From the global capacity curve shown in Figure 17 the calculated Life Safety performance level limit was located at 0.52 g spectral acceleration. The calculated spectral acceleration of 0.44 g and 0.43 g shown in Table 7 were still within the life safety performance level.

Performance level of Collapse Prevention hazard was limited at 0.98 g of spectral acceleration. The safe house structural survival capacity was very dependent on the earthquake time history and geological area. For example, the safe house structure is able to sustain 6.0 magnitude of Richter scale of Christ Church New Zealand earthquake on December 2011 and 7.3 magnitude of Richter scale of Chichi earthquake in Taiwan [18]. For Mercalli's scale [22], spectral acceleration between 0.65 g to 1.24 g was classified under class IX intensity with violent shaking and heavy damage toward the structures. Hence, the earthquake magnitude and intensity sustained by safe house can be calculated with the aid of spectral acceleration shown in Table 7.

Besides, Table 7 also summaries the structural global demand parameters from the entire data obtained from the laboratory test. The maximum storey drift and maximum base shear force from the experimental were shown in Table 7. The displacement ductility demands of the structure in both directions were calculated from the hysteresis curve shown in Figure 10, 11, 12 and 14. The displacement ductility demand of the structure was calculated by obtaining the roof top displacement (δ_{top}) and yielding point (δ_{yield}) of the structure in the first cycle load test. The yielding point of the structure from the experimental test was located at displacement of 6.36 mm with 3.4 kN base shear. The structure was in elastic state up to 6.36 mm storey drift without occurrence of permanent drift. When the structure was loaded up to 6.67 mm roof top displacement in the positive direction and unloaded back the recorded permanent drift of the structure was 0.2 mm for the first cycle load test. This explains the ductility demand in positive direction starts to become ductile with value of 1.05. The method of calculation was applied to subsequent cycles test.

Starting from third cycle load test the ductility of the structure from the experimental work was risen up to 3.99 with Collapse Prevention performance level. This is due to the rotation of concrete blocks during the experimental test. The rotation of several concrete blocks may contribute in increasing the roof top displacement. The rotation of concrete block was caused by imperfection in geometrical shape and eccentric load distribution from the roof top to every concrete blocks within the structure.

The ductility value was increased up to 7.72 in the fourth cycle test. This is due to the contribution from concrete cracks, spalling and crushing of concrete in every cycle load test. Ductility demands beyond 7.72 have the tendency of collapse or dislocation of structure.

Table 7 Safe house pushover cyclic load test summary

Cycle	Storey Drift (mm)		Displacement Ductility Demand (δ_{top} / δ_{yield})		Base shear force, V_g (kN)		Spectral acceleration ($S_a = V_g/W$)	
	direction		direction		direction		direction	
	+	–	+	–	+	–	+	–
1	6.67	6.36	1.05	1.00	2.6	3.4	0.26g	0.33g
2	12.7	12.69	2.00	1.99	4.5	4.4	0.44g	0.43g
3	25.43	25.29	3.99	3.97	5.9	7.3	0.58g	0.72g
4	49.09	47.62	7.72	7.49	9.9	9.1	0.98g	0.90g

5.0 CONCLUSIONS

The down-scaled 1:5 safe house model has ultimate capacity of 9.9 kN base shear force and 49.1 mm of roof top displacement. Behaviour of the safe house structure was identified from the pushover experimental test which included with rotation, separation and sliding of concrete blocks. Structural damages such as cracking, spalling, crushing of concrete cover, diagonal cracks on wall panels, formation of plastic hinge at beam to column joint

and failure of foundation were recorded in the experimental test.

For structural stiffness capacity, the safe house has effective stiffness capacity of 0.3 kN/mm in both directions test. The obtained post yielding structural stiffness in negative direction was 0.08 kN/mm. The calculated post yielding structural stiffness in positive direction test was 0.14 kN/mm. The effective stiffness capacity for two bays two storeys safe house pushed in both directions were the same. The structure has maximum displacement ductility of 3.90. The safe house structure has the tendency of collapse if the displacement ductility exceed 7.72 caused by a higher earthquake loads.

The recorded maximum energy dissipation in the first cycle test was 3.1 kNmm for the negative direction test. Similarly, maximum seismic energy of 21.5 kNmm was dissipated in negative direction for the second cycle test. In third cycle test, the recorded highest seismic energy dissipation of 62.0 kNmm was from positive direction test.

The safe house structural system has Immediate Occupancy performance level to resist earthquakes with 0.33 g of spectral acceleration. The structure can sustain 0.52 g of spectral acceleration from earthquakes in Life Safety performance level. Ultimately the structure was able to sustain the earthquake impact up to performance level Collapse Prevention of 0.98 g which is equivalent to 6.0 magnitudes of Richter scale or within class IX intensity by Mercalli's scale. The safe house structure would have total collapse hazard beyond the spectral acceleration of 0.98 g.

This concludes the safe house has ability to dissipate seismic energy and sustained earthquake hazard up to 0.98 g of force.

Acknowledgement

This research was supported by UTM-URG-QJ130000.2522.05H06, Elastic Infills, Beams and Column for Natural Disaster Resistance House.

References

[1] Guha-Sapir, D., Hoyois, Ph. and Below. R. 2012. Annual Disaster Statistical Review 2012 – The Numbers and Trends. Report of Epidemiology of Disasters, Institute of Health and Society: 1-50.

[2] National Earthquake Information Center. 2012. M8.6 & M8.2 Northern Sumatra Indonesia Earthquakes of 11 April 2012. [Earthquake Summary Map]. Global Seismographic Network: Department of the Interior & Geological Survey, United State.

[3] Jacques, B. M. 2008. *Seismic Engineering*. John Wiley & Sons, Inc., 111 River Street Hoboken, NJ 07030, USA.

[4] Sinchuan Earthquake Death Toll Exceeds 21500 & 14000 Others Remain Buried. (2008, 16th May). Chinaviewnews, Retrieved December 26, 2011, from http://news.xinhuanet.com/english/2008-05/16/content_8187277.htm.

[5] Balendra, T. and Li, Z. 2008. Seismic Hazard of Singapore and Malaysia. *EJSE. Special Issue: Earthquake engineering in the low and moderate seismic regions of Southeast Asia and Australia*. 57-63.

[6] Nasim, U. and Uday, V. 2005. Ballistic Testing of Polymer Composites to Manufacture Emergency Safe House Shelters. *Journal of Composites for Construction.* 9(4): 369-375.

[7] Nur, Y., Tanya, T. and Danny, K. 2005. Hurricane Wind Shelter Retrofit Room Guidelines for Existing Houses. *Practice Periodical on Structural Design and Construction.* 10(4): 246-252. ASCE–American Society of Civil Engineers.

[8] Lu, G. Y., Zhang, G. Q. and Han, Z. J. 2010. Design and Optimization of an Emergency Shelter. Journal of Applied Mechanics and biomechanics, 978-1-4244-7739-5/10/2010, 1-4. IEEE–Institute of Applied Mechanics and Biomechanics.

[9] Brandford, N. M. and Sen, R. 2005. Multi Parameter Assessment Guide for Emergency Shelter: Disaster Relief Applications. *Journal of Performance of Constructed Facilities*. 19(2).

[10] Federal Emergency Management Agency. 2014. FEMA 320 Taking Shelter from the Storm: Building a Safe Room for Your Home, Washington, D.C.: Department of Homeland Security.

[11] Andrew, B., Mohammed, Z., Long, Q. and Phelan, R. S. 2006. Validation of Finite Element Analyses for Storm Shelters. *Journal of Architectural Engineering*. 12(2).

[12] Helmut, K. and Eduardo, M. 2004. Performance Based Earthquake Engineering. Earthquake Engineering from Engineering Seismology to Performance-Based Engineering. 9.1-9.5.

[13] Majid, A., Romain, B. and Nawawi, C. 2013. Dynamic Response of Mortar-Free Interlocking Structures. *Journal of Construction and Building Materials*. 42: 168-189.

[14] Federal Emergency Management Agency. 1996. FEMA 273 NEHRP Guidelines for the Seismic Rehabilitation of Building. Building Safety Seismic Council, Washington, D.C.: Department of Homeland Security.

[15] Federal Emergency Management Agency. 2000. FEMA 356 Pre-standard and Commentary for the Seismic Rehabilitation of Building. Washington, D.C.: Department of Homeland Security.

[16] Federal Emergency Management Agency. 2005. FEMA 440 Improvements of Nonlinear Static Seismic Analysis Procedures. Washington, D.C.: Department of Homeland Security.

[17] Matthew, J. S. 2000. Reliability-Based Seismic Performance Evaluation of Steel Frame Buildings using Nonlinear Static Analysis Methods. *Journal of Construction and Building Materials, University Of California, Los Angeles*.

[18] USGS. 2013. Historic World Earthquakes, United State National Earthquake Information Center. Retrieved December, 2013, from http://earthquake.usgs.gov/earthquakes/world/historical.php/.

[19] British Standard Institution. 1992. European code 3: Design of Steel Structure. London: British Standards Institution.

[20] British Standard Institution. 2000. B.S. 5950: Structural Use of Steelwork in Building. London: British Standards Institution.

[21] British Standard Institution. 1996. B.S. 6399: Loading for Buildings. London: British Standards Institution.

[22] Jones, T. 2003. Chapter 4: Earthquake Risks. Geosciences Australia, Canberra, Australia. 46-70.